Solar Energy Materials & Solar Cells 161 (2017) 62–69

Contents lists available at ScienceDirect

Solar Energy Materials & Solar Cells

journal homepage: www.elsevier.com/locate/solmat

Experimental study of using both ZnO/ water nanofluid and phase change material (PCM) in photovoltaic thermal systems

Mohammad Sardarabadi, Mohammad Passandideh-Fard*, Mohammad-Javad Maghrebi, Mohsen Ghazikhani

Department of Mechanical Engineering, Air and Solar Research Institute, Ferdowsi University of Mashhad, Mashhad, Iran

ARTICLE INFO

Keywords:
Photovoltaic thermal system
Phase change material
Nanofluid
Electrical and thermal efficiency

ABSTRACT

In this study, the effects of simultaneous use of a *ZnO*/water nanofluid and a phase change material (PCM) as coolant mediums for a photovoltaic (PV) fluid/nanofluid based collector system are investigated experimentally. By designing and fabricating two similar photovoltaic thermal systems, one with a PCM medium (PVT/PCM) and one without a PCM (PVT), the experiments are performed. The measured results for surface temperature, thermal and electrical efficiency of the systems are compared with each other and with those of a conventional photovoltaic module as a reference system based on a thermodynamic viewpoint. In addition, the results for a nanofluid as a working fluid is compared with those using pure deionized water. Results show that in the PCM/nanofluid based collector system, the average electrical output is increased by more than 13% compared to that of the conventional PV module. Using a nanofluid, instead of deionized water, improved the average thermal output by nearly 5% for the PVT system; when the PCM was also employed (i.e., for the PVT/PCM system) the increase in the thermal efficiency was nearly 9% without any extra energy consumption. Based on the results of an exergy analysis, the simultaneous use of both a nanofluid and the PCM for the cooling system, increases the overall exergy efficiency of the system more than 23% compared to that of a conventional PV module.

1. Introduction

A conventional photovoltaic module (PV) consists of silicon cells that directly convert the solar energy to electricity. Since all photons from the solar spectrum do not have sufficient energy to produce electricity in the cells and the process of electricity generation in these cells is exothermic, the temperature of the cells will increase. Increasing the cell temperature decreases the open circuit voltage and, thus, reduces the electrical efficiency of the PV module [1]. Increasing the thermal capacitance is a useful technique for limiting temperature increases. One effective method of increasing thermal capacitance and whereby controlling the temperature, is the use of a phase change material (PCM) at a desired temperature. Paraffin is available in a wide range of melting points. Organic paraffin as one type of these materials, is non-hazardous and affordable. In addition, it has a certain phase change temperature and its thermo-physical properties remain unchanged over many freeze/melt cycles. Therefore, organic paraffin can be used as a cooling medium in mechanical systems. The PCM not only keeps the cells cool, it stores the excess solar power for a later use. This feature leads to a steady and uniform thermal output during the working period of solar power systems. In recent years, several experimental, analytical and numerical studies have been performed to integrate photovoltaic modules with the PCMs. Hasan et al. [2] experimentally evaluated the use of the PCM for the thermal regulation enhancement of a building equipped with PV modules. They selected five different PCMs with a melting temperature of around 25 °C for the use in four different PV/PCM systems. Based on their experiments at 1000 W/m^2 solar radiation, a maximum temperature reduction of 18 °C can be achieved by integrating the PV module with the PCM. For the steady condition, the temperature reduction was about 10 °C. Huang et al. [3] experimentally evaluated and analyzed the effects of convection and crystalline segregation in a PCM as a function of thermal efficiency within a finned PV/PCM system. They concluded that the fins effectively moderate the temperature rise of the front surface of the PV/PCM system. In another work, Hasan et al. [4] investigated the performance improvement of PV modules by using the PCM to regulate the cell temperature in various climate conditions, both numerically and experimentally. They indicated that regardless of the type of the PCM, such systems are only effective in hot and stable climatic conditions. A complete review of using PCMs as a thermal regulation in PV modules can be seen in the works of Ma et al. [5] and Browne et al. [6].

* Corresponding author.
E-mail address: mpfard@um.ac.ir (M. Passandideh-Fard).

http://dx.doi.org/10.1016/j.solmat.2016.11.032
Received 9 June 2016; Received in revised form 19 November 2016; Accepted 24 November 2016

Nomenclature

Abbreviations

A	Area (m2)
C_p	Specific heat (J/kg. K)
E	Energy (J)
Ex	Exergy (J)
FF	Filled factor (dimensionless)
G	Incident solar irradiation (W/m2)
I	Electrical current (A)
PCM	Phase Cnange Material
PF	Packing factor (dimensionless)
PV	Photovoltaic module
PVT	Photovoltaic thermal system
PVT/PCM	PVT system equipped by PCM collector
T	Temperature (K or °C)
V	Voltage (V)
wt	Weight (kg)
ZnO	Zinc oxide

Greeks

α	Absorptivity
β	Half-angle of the cone subtended by the sun's disc
τ	Transitivity
δ	Uncertainty
ε	Exergetic efficiency
η	Energetic efficiency
ρ	Density
ϕ	Volumetric ratio
v	Arbitrary parameter

Subscripts

amb	Ambient
c	Collector
$cell$	Photovoltaic cell
eff	Effective
el	Electrical
eqp	Equipment
f	Fluid
in	Input
$loss$	Losses
m	Mass weigh
n	Nanoparticle
nf	Nanofluid
oc	Open circuit
o, f	Outlet of the fluid
out	Outlet
sc	Short circuit
th	Thermal

Another effective method for the thermal regulation of PV modules is adding a thermal collector to recover the extra generated heat in the system. This combined system is known as a photovoltaic thermal system (PVT) which can generate electricity and useful thermal energy, simultaneously. In addition, the thermal recovery in a PVT system leads to a temperature reduction of PV cells resulting in an increase of the electrical efficiency. The PVT systems are divided in various categories depending on the collector type (such as sheet and tube [7] and heat pipes [8]), working fluid (such as air based [9] and water based [10]), and the cell cover (glazed or unglazed [11]). For a PVT system, the working fluid can be changed in order to improve its overall performance. Using a liquid as working fluid results in a higher thermal capacitance in the system which in turn causes more cooling. In addition, by using liquid coolants, useful thermal energy is under control that can be used for different applications such as preheating water. Water with a high thermal capacity is a conventional working fluid for the PVT systems. Improving the thermal properties of the working fluid, however, may be considered an effective way to increase the performance of these systems.

Recently, the nanofluid technology has created a new concept in solar applications [12], especially for the PVT systems. Michael and Iniyan [13] performed an analysis of using a copper oxide/water nanofluid as the working fluid in a PVT system. They concluded from the experiments that the copper oxide/water nanofluid can make a significant improvement in the thermal performance of the PVT system. Moreover, they mentioned that using a good heat exchanger can improve the electrical performance. Ghadiri et al. [14] investigated the thermal and electrical output of a PVT system by nano-ferrofluids coolants under constant and alternating magnetic fields. They used a solar radiation simulator for their experiments performed in the laboratory. Their experiments showed 79% improvement in the overall efficiency (electrical and thermal) of the system. Rejeb et al. [15] studied numerically the use of different nanofluids and base fluids on the efficiency of an uncovered PVT equipped with a sheet and tube nanofluid based collector. They validated the numerical results with those of the experiments. They considered the aluminum and copper

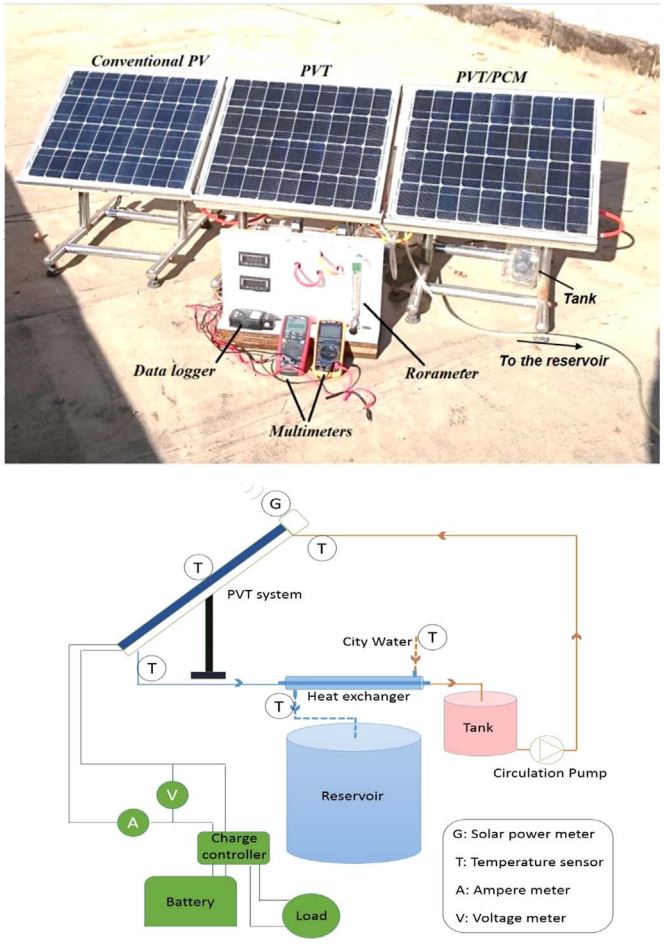

Fig. 1. A view and schematic diagram of the experimental setups.

Table 1
Thermophysical properties of nanoparticles and phase change material.

Nanoparticles		Phase change material (PCM)	
Type	Zinc-oxide	Type	Paraffin wax (Merck)
Particle size	35–45 nm	Melting point	42–72 °C
Conductivity	23.4 W/mK	Solidification point	46–48 °C
Quantity	0.2 wt% of base fluid	Quantity	2 kg
Purity	99+ %	Packing factor	0.5
Density	5606 kg/m^3	Density	900 kg/m^3 (20 °C)
Specific heat	0.514 kJ/kg. K	Specific heat capacity	2.14–2.9 kJ/kg. K[18]
		Heat of fusion	200–220 kJ/kg[18]

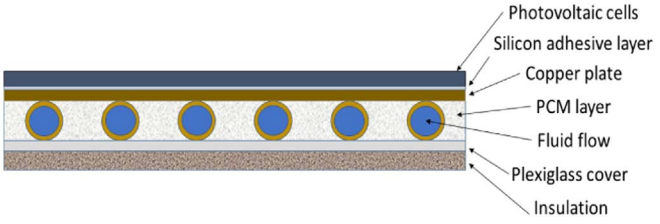

Fig. 2. A cross section view of the PVT/PCM setup.

Table 2
Characteristics of the selected equipment of PVT system.

PV modules		Thermal collectors	
Cells type	Mono-crystalline silicone	Type	Copper sheet and tube
Cells dimension	62.5*125 mm	Dimension	630*540 mm
Number of cells	36	Number of tubes	16
Module dimension	630*540*28 mm	Tube diameter	10 mm
Packing factor	0.83	Packing factor	1
Open circuit voltage	21.60 V		
Short circuit current	2.57 A	**Batteries**	
Maximum output power	40 W	Type	Sealed lead
Module efficiency	15%	Initial current	2.16 A
		Voltage range	13.5 up to 15 V
Insulation		Power	28 W
Type	Rigid polyurethane foam		
Thickness	30 mm		
Thermal conductivity	0.025 W/(m. K)		
Density	30 kg/m^3		
Specific heat capacity	1.5 kJ/(kg. K)		

oxides nanoparticle with three different mass fractions (0.1, 0.2 and 0.4 wt%). They indicated that using the deionized water as a base fluid provides a higher performance compared to that of the ethylene glycol. Furthermore, using CuO/water as a coolant for the PVT system, resulted in the best thermal and electrical efficiency. More details of using nanofluids in solar systems and their effects on the system performance can be seen in the study of Verma and Tiwari [16] and Najah Al-Shamani et al. [17].

There is a large volume of published studies describing the use of a fluid or a PCM based cooling, separately. The simultaneous use of these methods can be a suitable technique for improving the overall efficiency (thermal and electrical efficiency) of the PVT system. The research on this topic is rare in the literature. The present studyfocuses

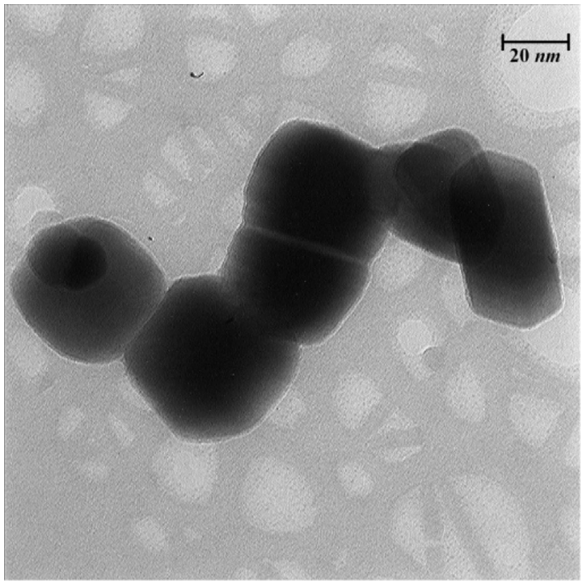

Fig. 3. TEM of ZnO nanoparticles (taken in central laboratory of the Ferdowsi University of Mashhad).

on the effects of using a fluid/nanofluid based collector with and withouta PCM medium, experimentally. Selected fluids are pure deionized water and ZnO/water nanofluid. An organic paraffin wax is alsoselected as the PCM medium. The results of electrical and thermal outputs are compared with each other and with those of a conventional photovoltaic module from both the first and second law of thermodynamics viewpoints.

2. Experimental setup

A view and schematic diagram of the experimental setups are shown in Fig. 1. There are three different setups in the experiments all consisting of a 40 W monocrystalline silicon photovoltaic module (Suntech Co., China). The first system, referred as PV, is a conventional photovoltaic module without any external cooling system. In the second system, referred as PVT, the photovoltaic module is equipped with a copper sheet and tube collector. The third system is similar to that of the second system, however, the tubes are surrounded by two kilograms of paraffin wax (MERCK, 107151) as the PCM (thermos-physical properties of the selected PCM can be seen in Table 1); this system is referred as PVT/PCM. A cross section of the PVT/PCM collector is shown in Fig. 2. All systems are tested in exactly the same conditions. Selected equipment charactristics of the PVT system is

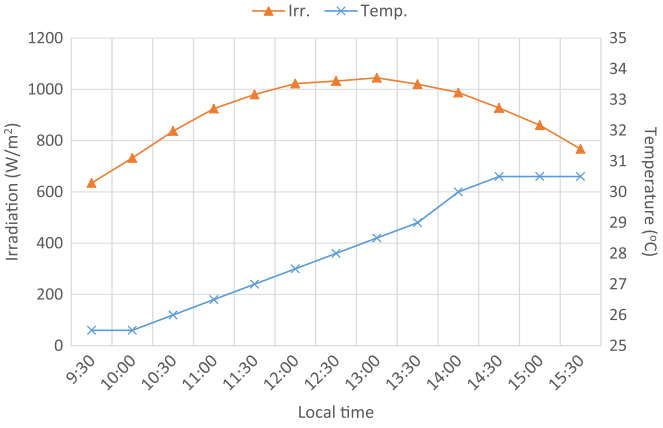

Fig. 4. The average solar irradiation and ambient temperature during the experimental period.

given in Table 2.

In the PVT and PVT/PCM setups, a shell and tube heat exchanger is used to cool the working fluids in a closed flow circuit after having absorbed the heat in the collectors. A working fluid with a mass flow rate of 30 kg/h is used in each PVT (and PVT/PCM) system. The details of the selection procedure for the fluids mass flow rate can be seen elsewhere [1]. The second fluid used in the shell and tube heat exchanger is the running city water (with a mass flow rate of 40 kg/h) stored in a tank as preheated water. The working fluids considered in the experiments are distilled water and a zinc-oxide (*ZnO*)/water nanofluid. Nanoparticles have been purchased in the powder form (US Research Nanomaterials, Inc.). *ZnO* nanoparticles, under 50 *nm* in diameter (see Fig. 3), are dispersed in water by 0.2% wt. and stabilized with an ultrasound mechanism and acetic acid (*CH3COOH*) as a surfactant. The ZnO (Table 1) is selected as a favorite metal oxide nanoparticle due to its relatively high thermal conductivity. Moreover, this nanoparticle shows more stability in the base fluid in comparison with other tested metal oxides (including copper oxide, aluminum oxide and titanium oxide). The daily measured data was collected from 9:30 am to 3:30 pm on selected days in August and September at the Ferdowsi University of Mashhad, Mashhad, Iran (Latitude: 36° and Longitude: 59°). In the experiments, the tilt angle of the collector was set at a constant value of 30 degrees (the slope with respect to the horizontal surface while the collector is facing south).

In order to examine the nanofluid stability, its density is measured several times during the experiment where no significant changes were observed. No sedimentation of nanoparticles in the suspension was observed after 7 days. Fluid flow temperatures at the inlet and outlet of the heat exchanger and that of the collector are measured by K-type sensors. The collected data are then stored by a data logger (Testo, 177 T4). The surface temperature of different points (middle and four corners) of the PV unit are measured by a portable K-type surface thermocouple where the maximum value is reported as the PV surface temperature. Digital multimeters are used to measure the short-circuit and load currents, and the open-circuit and load voltages. The total incident radiation is measured by a solar power meter (TES-1333) positioned parallel to the photovoltaic surfaces. The working fluid mass flow rates are controlled and measured by a rotary flow meter. More details of the measuring instruments and experimental uncertainties can be found elsewhere [1].

The experiments are performed in selected days of August and September 2016. The average incident solar irradiation to the PV surfaces and the average ambient temperature during the experimental period are shown in Fig. 4.

3. Thermodynamic analysis

The electrical and thermal energies are the outputs of a PVT system. By considering the PV module and the thermal collector as a combined control volume, the energy balance for this control volume, can be expressed as:

$$\dot{E}_{in} = \dot{E}_{el} + \dot{E}_{th} + \dot{E}_{st} + \dot{E}_{loss} \quad (1)$$

where $\dot{E}_{in}$ is the incident solar irradiation; $\dot{E}_{el}$ the output electrical power; $\dot{E}_{th}$ the useful thermal energy gained from the collector; $\dot{E}_{st}$ the amount of the stored energy in the PCM and other parts of the system; and $\dot{E}_{loss}$ is the energy losses from the control volume.

The overall efficiency can be expressed as:

$$\eta_{pvt} \cong \frac{\dot{E}_{th} + \dot{E}_{el}}{\dot{E}_{in}} \Rightarrow \eta_{pvt} = \eta_{th} + r.\ \eta_{el} \quad (2)$$

where A_c and A_{pv} are the area of the collector and PV cells, respectively, and r is the packing factor defined as A_{pv}/A_c. $\dot{E}_{th}$ can be calculated as:

$$\dot{E}_{th} = \dot{m}_f.\ C_{p,f}.\ (T_{f,o} - T_{f,i}) \quad (3)$$

where $\dot{m}_f$ is the fluid mass flow rate through the collector, $C_{p,f}$ the fluid specific heat, $T_{f,i}$and $T_{f,o}$represent the fluid inlet and outlet temperatures, respectively. The thermo-physical properties of the prepared nanofluid can be calculated from water and nanoparticle characteristics at the bulk temperature using following equations [1]:

$$C_{p,nf} = \frac{\phi.\ (\rho_n.\ C_{p,n}) + (1 - \phi).\ (\rho_f C_{p,f})}{\rho_{nf}} \quad (4)$$

$$\rho_{nf} = \phi.\ \rho_n + (1 - \phi).\ \rho_f \quad (5)$$

whereρ is the density and subscripts n, f and nf represent, the nanoparticle, fluid, and nanofluid, respectively. ϕ is the volumetric ratio of the nanoparticle in the base fluid that can be calculated as:

$$\phi = \frac{m_n/\rho_n}{m_n/\rho_n + m_f/\rho_f} \quad (6)$$

where $m_n$and m_f are the mass of the nanoparticle and the fluid, respectively.

The electrical efficiency can be expressed as:

$$\eta_{el} = \frac{\dot{E}_{el}}{\dot{E}_{in}} = \frac{V_{oc} \times I_{sc} \times FF}{G_{eff}} \quad (7)$$

where V_{oc} is the measured open circuit voltage, I_{sc} the measured short circuit current and $\dot{G}_{eff}$is the effective absorbed solar irradiation by the PV module. FF is the filled factor defined as the maximum power conversion efficiency of the PV unit and is expressed as a function of the cell temperature (T) [19] as:

$$FF = f\,(V_{oc}/T) \quad (8)$$

As a result, the electrical efficiency of the PV module is inversely proportional to the cell temperature. Thus, the increase of the cell temperature results in a reduction of the system electrical output power and vice versa (the details of the electrical efficiency calculation can be seen elsewhere [1]).

In order to analyze the PVT system based on the thermal energy, the output electrical energy must be converted into thermal energy for which a conversion factor c_f has been used in the literature as:

Table 3
Measuring equipment and their uncertainties.

Equipment and model	Measurement section	Accuracy	Maximum uncertainty (in experiments)
Digital multimeter-UT71C/D/E	Voltage (Open circuit and load)	±(0.5% + 1)	0.06 V
Digital multimeter-UT71C/D/E	Ampere (short circuit and load)	±(0.8% + 1)	0.02 A
Pyranometer-TES1333	Incident solar radiation	$\pm\ 10W/m^2$ + $0.38W/m^2\,(for\,T_{ref} + 1^oC)$	5.8 W/m^2
K-types thermocouple	PV surface temperature	$\pm 0.25^{\circ}C$	0.14 °C
RTD and PT100 thermocouple	Fluid temperatures	$\pm 0.15^{\circ}C$ *to* $\pm 0.25^{\circ}C$	0.14 °C
Hg thermometer	Ambient temperature	$\pm 0.5^{\circ}C$	0.3 °C
Rotameter-LZB10	Mass flow rate	$\pm 2kg/hr$	1.15 kg/h

$$\dot{E}_{el,th} = \frac{\dot{E}_{el}}{c_f} \tag{9}$$

For the most PVT fluid systems, a value of c_f between 0.35 and 0.40 has been introduced [1]; in this study, a value of 0.38 was used in the analysis.

It should be noted that the quality of an equal amount of electrical and thermal energies from a thermodynamic viewpoint are not considered to be the same. The thermal energy cannot be converted to the useful work until there is a temperature difference between two thermal reservoirs. On the other hand, the entire electrical energy is regarded a useful available work. Therefore, considering the differences between these two outputs (thermal and electrical) is an important factor in analyzing a PVT system. The exergy analysis based on the 2nd law of thermodynamics is required to determine the performance of the PVT systems because it is more realistic and it considers the quality of energies as well. Similar to the energy analysis, by considering the photovoltaic module and the thermal collector as a combined control volume, the result of the exergy balance equation can be written as:

$$\dot{E}x_{in} = \dot{E}x_{el} + \dot{E}x_{th} + \dot{E}x_{st} + \dot{E}x_{loss} \tag{10}$$

Various terms in this equation are defined similar to those of the energy balance (Eq. (1)) but in an exergy expression.

Similar to Eq. (2), the overall exergetic efficiency of the PVT system can be calculated based on the following expression [1]:

$$\varepsilon_{pvt} \cong \frac{\dot{E}x_{th} + \dot{E}x_{el}}{\dot{E}x_{in}} = \varepsilon_{th} + r\varepsilon_{el} \tag{11}$$

where ε_{pvt} is the overall exergetic efficiency, $\varepsilon_{th}$the thermal exergetic efficiency and $\varepsilon_{el}$is the electrical exergetic efficiency. $\dot{E}x''_{th}$is the rate of output thermal exergy per unit collector area, $\dot{E}x''_{el}$ the rate of output electrical exergy per unit area of the photovoltaic cells and $\dot{E}x''_{in}$is the rate of the incident radiation exergy.

In Eq. (11), the thermal and electrical output exergies are related to the output energies as [1]:

$$\dot{E}x_{el} = \dot{E}_{el} \tag{12}$$

$$\dot{E}x_{th} = \dot{E}_{th}\left(1 - \frac{T_{amb}}{T_{f,out}}\right) \tag{13}$$

where all temperatures are in Kelvin and $T_a$is the ambient temperature. The input exergy from the sun can be evaluated as follows [20]:

$$\dot{E}x_{in} = \dot{E}x_{sun} = \dot{G}_{eff}\left[1 - \frac{4}{3}\frac{T_{amb}}{T_{sun}}(1 - \cos\beta)^{1/4} + \frac{1}{3}\left(\frac{T_{amb}}{T_{sun}}\right)^4\right] \tag{14}$$

where T_{sun} is the equivalent temperature of the sun as a blackbody ($\cong 5800K$) and $\beta$is the half-angle of the cone subtended by the sun disc. In this study, a diffuse sunlight ($\beta \cong \pi/2$) is used in the calculations.

4. Uncertainty analysis

An uncertainty analysis is performed on both thermal and electrical efficiencies from the first and second laws of thermodynamics viewpoints. The uncertainties associated with the measuring instruments of the experimental setup are reported in Table 3.

If R is a function of 'n' independent linear parameters as $R = R(v_1, v_2, v_3 \ldots v_n)$, the uncertainty of function R may be calculated as [21]:

$$\delta R = \sqrt{\left(\frac{\partial R}{\partial v_1}\delta v_1\right)^2 + \left(\frac{\partial R}{\partial v_2}\delta v_2\right)^2 + \ldots + \left(\frac{\partial R}{\partial v_n}\delta v_n\right)^2} \tag{15}$$

where δR is the uncertainty of function R, δv_i the uncertainty of parameter v_i, and $\frac{\partial R}{\partial v_i}$ is the partial derivative of R with respect to parameter v_i. Suppose that the parameters $v_1, v_2, \ldots, v_m, v_{m+1}, \ldots, v_n$ are measured with the uncertainties $\delta v_1, \delta v_2, \ldots, \delta v_m, \delta v_{m+1}, \ldots, \delta v_n$, and the function R is defined as:

$$R = \frac{v_1 \times v_2 \times \ldots \times v_m}{v_{m+1} \times \ldots \times v_n} \tag{16}$$

If the uncertainties in $v_1, v_2, \ldots, v_m, v_{m+1}, \ldots, v_n$ are independent, then the fractional uncertainty of R is written as [22]:

$$\frac{\delta R}{R} = \sqrt{\left(\frac{\delta v_1}{v_1}\right)^2 + \left(\frac{\delta v_2}{v_2}\right)^2 + \ldots + \left(\frac{\delta v_m}{v_m}\right)^2 + \left(-\frac{\delta v_{m+1}}{v_{m+1}}\right)^2 + \ldots + \left(-\frac{\delta v_n}{v_n}\right)^2} \tag{17}$$

Using the above equation (Eq. (17)) and recalling Eqs. (3), (7) and (12)–(14); fractional uncertainties of the sun input and the thermal/electrical outputs, from both energetic and exergetic viewpoints can be calculated. As an example, the electrical efficiency is a function of G and P_{el} (Eq. (8)); therefore, the maximum fractional uncertainty of the electrical efficiency can be calculated by considering the maximum uncertainties for each parameter based on the following equation:

$$\eta_{el} = f(G, P_{el}) \Rightarrow \frac{\delta\eta_{el}}{\eta_{el}} = \pm\sqrt{\left(\frac{\delta V}{V}\right)^2 + \left(\frac{\delta I}{I}\right)^2 + \left(\frac{-\delta G}{G}\right)^2} = \pm 0.017 \tag{18}$$

which means that the maximum uncertainty of the electrical efficiency in the experiments is 1.7%. Using a similar method, the uncertainties for other functions can be calculated as well. The results of this analysis are presented in Table 4 where it can be seen that the maximum absolute uncertainty for all parameters is less than 3% in the experiments. This is an indication of the reliability of the measured data.

5. Results and discussion

In the present study, electrical and thermal outputs of the PVT systems are selected as the essential parameters of the systems when comparing the results. The results of the measurements are compared with each other from the viewpoint of both first and second laws of thermodynamics.

5.1. Surface temperature

To investigate the effect of PV cooling on the surface temperature reduction, the surface temperature of three systems is measured each 30 min during the experimental period. The maximum measured values are shown in Figs. 5 and 6 as the PV surface temperature, for deionized water and nanofluid based collectors, respectively.

As observed in these figures (Figs. 5 and 6), by using a fluid (deionized water or nanofluid) as the coolant of the PVT system, the maximum surface temperature can be reduced nearly 10 degrees (in average) compared to that of the conventional PV module. However, the difference between nanofluid and deionized water in temperature reduction is negligible. The surface temperature of the nanofluid based system is about one degree cooler than that of the deionized water based collector in both the PVT and PVT/PCM. Furthermore, adding a PCM to the cooling system of the PVT (i.e., PVT/PCM) not only results in a more temperature reduction (in average, more than 6 degrees cooler than that of a PVT fluid based system) but also causes a more stable surface temperature during the day. Moreover, the melting point of the PCM can be a limitation factor for the overall temperature

Table 4
Fractional uncertainties of the exergy and energy equations.

$\delta\dot{E}_{sun}/\dot{E}_{sun}$	$\delta\dot{E}_{el}/\dot{E}_{el}$	$\delta\dot{E}_{th}/\dot{E}_{th}$
$f(G)$	$f(V, I, G)$	$f(G, \dot{m}, c_p, T_{in}, T_{out})$
Eq. (1).	Eq. (7).	Eqs. (2) and (3).
Fig. 4	Figs. 7 and 8	Figs. 9 and 10
±0.009	±0.017	±0.028

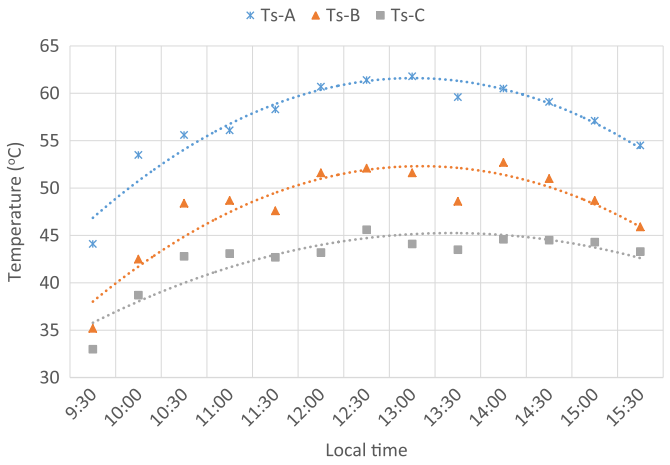

Fig. 5. Photovoltaic surface temperature variation during the experimental period for (A) Conventional PV, (B) PVT water based collector and (C) PVT water/ PCM based collector.

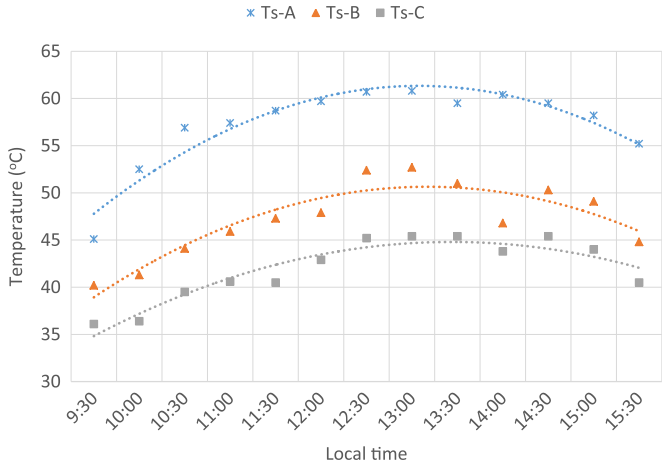

Fig. 6. Photovoltaic surface temperature variation during the experimental period for (A) Conventional PV, (B) PVT nanofluid based collector and (C) PVT nanofluid/ PCM based collector.

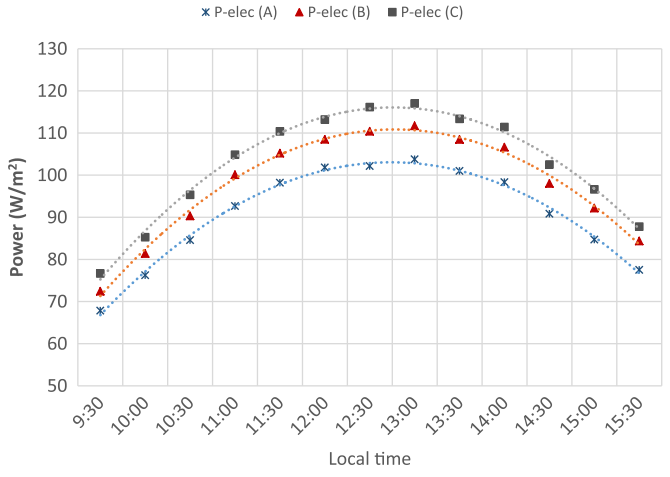

Fig. 7. Electrical output power variation during the experimental period for (A) Conventional PV, (B) PVT water based collector and (C) PVT water/ PCM based collector.

increases of the system.

5.2. Electrical output

The most important parameter in a PVT system is the electrical

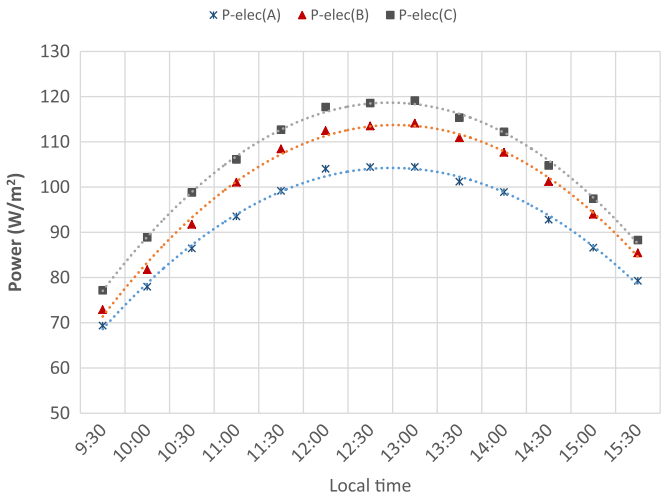

Fig. 8. Electrical output power variation during the experimental period for (A) Conventional PV, (B) PVT nanofluid based collector and (C) PVT nanofluid/ PCM based collector.

Table 5
Average electrical output power (W/m^2).

PV	92.16	92.16
	Deionized water	*ZnO*/water
PVT	99.24	99.63
PVT/PCM	103.99	104.4

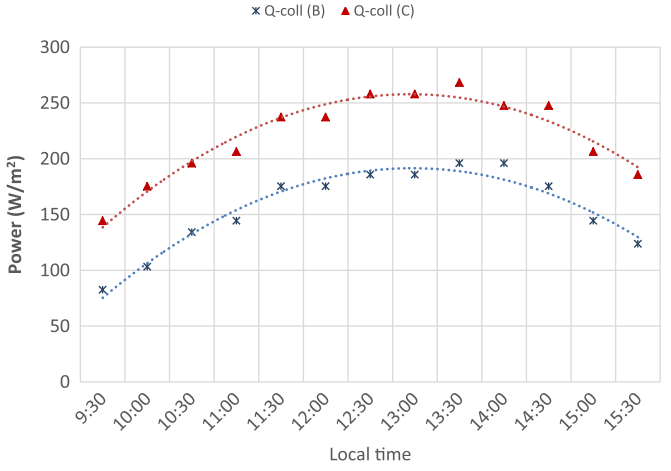

Fig. 9. Thermal output power variation during the experimental period for (B) PVT water based collector and (C) PVT water/ PCM based collector.

output which is vital in finding whether a system configuration is efficient. The electrical output power of the entire cases considered in this study are shown in Figs. 7 and 8, for the deionized water and nanofluid based collectors, respectively.

Based on Eqs. (7) and (8), the electrical output power is reversely related to the PV cell temperature. The results of the measurements and the system analysis for the electrical output during the experimental period (9:30 am –15:30 pm) (Figs. 7 and 8) are summarized in Table 5.

Although the difference between water based and nanofluid based collectors is negligible for both the PVT and PVT/PCM, using a fluid based and especially a PCM/fluid based collector considerably increases the electrical output. As an example in the PVT/PCM, the average electrical output is increased by more than 13% compared to that of the conventional PV module.

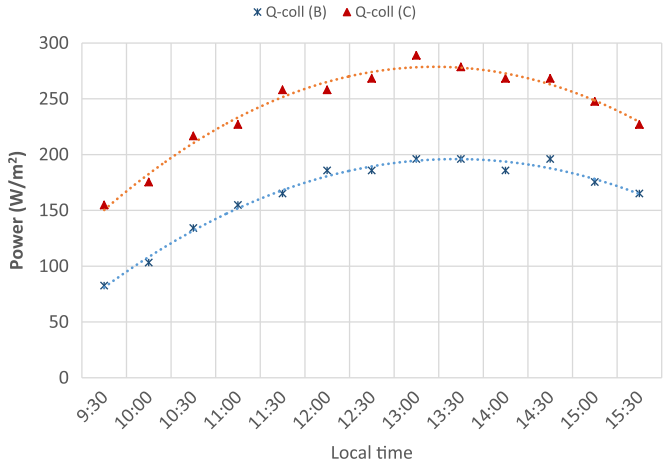

Fig. 10. Thermal output power variation during the experimental period for (B) PVT nanofluid based collector and (C) PVT nanofluid/ PCM based collector.

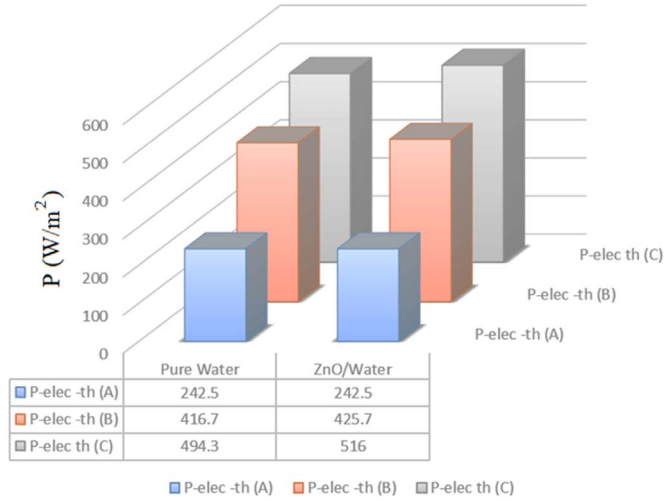

Fig. 11. Equivalent thermal-electrical power output (W/m^2) for (A) Conventional PV, (B) PVT nanofluid based collector and (C) PVT nanofluid/ PCM based collector.

5.3. Thermal output

The useful thermal energy output of the PVT system, indicates the amount of the absorbed heat by the cooling fluid in the collector. In this study, the thermal energy is evaluated based on both energy and exergy approaches for the PVT and PVT/PCM cases compared to each other and to those of a conventional PV module. Furthermore, by converting the electrical energy of the system to a useful thermal energy (Eq. (9)), all three setup configurations (the conventional PV, PVT and PVT/PCM) are compared with each other from the energy point of view.

The results of the thermal energy output of the systems, calculated based on Eq. (3), can be seen in Figs. 9 and 10, for deionized water and nanofluid based collectors, respectively.

The thermal energy results show that using a PCM/fluid based collector can increase the thermal output, considerably. As a result, the average thermal energy output for the case of a PCM/water based collector is increased by 42% compared to that of a water based collector. This value is about 48% for the case of a PCM/nanofluid based collector compared to that of a nanofluid based collector. Using the nanofluid instead of deionized water improves the average thermal output by about 5% and 9% for the case of fluid and PCM/fluid based collectors, respectively. Based on the thermal output results of the systems, the PCM can significantly increase the specific heat of the PVT system, which in turn, translates into less thermal losses from the panel and less temperature fluctuations. Therefore, using the PCM makes the system to be economically justified. Nanoparticles can increase the working fluid thermal conductivity. By adding nanoparticles to the base fluid, the heat transfer of the fluid flow to the PCM and also to the heat exchanger can be increased.

By converting the electrical output to the useful thermal energy (using Eq. (9)), all systems can be compared with each other from the equivalent energy viewpoint. The daily average results for the experimental conditions are shown in Fig. 11.

It is seen from Fig. 11 that by using a fluid-type heat recovery system (PVT), the equivalent electrical-thermal output energy of the system can be increased more than 1.7 times in comparison with a conventional photovoltaic module. Also, the simultaneous use of a fluid and a PCM medium increases the equivalent electrical-thermal outputs to more than two times. It should be mentioned that because of the aggregation of the electrical and thermal outputs, the nanofluid based collector has a negligible effect on this parameter in comparison with the deionized water based collector.

In order to examine the quality of the output energy of the systems, all systems outputs are compared based on an exergetic analysis. Based on Eq. (11), the overall exergy efficiency of three mentioned systems and the average daily output exergy are reported in Table 6.

Based on the exergy results, the maximum overall exergy efficiency increase is for the simultaneous use of both nanofluid and PCM medium coolants. This configuration can increase the overall exergy efficiency by more than 23% compared to that of a conventional PV system. The main impact of using the PCM can be seen in the thermal exergy output of the system. The thermal exergy output can be increased by nearly twice when the PCM based collector is used. As a result, in addition to the positive effect of using a nanofluid based collector, employing a PCM medium can increase the overall exergy efficiency of the system without any extra power consumption. It should be noted that the PCM/water based collector even leads to a more exergy efficiency than that of the nanofluid based collector (PVT/nanofluid).

6. Conclusion

In this study, by designing and fabricating two PVT and PVT/PCM systems, the positive effects of using these collectors as cooling systems for a photovoltaic module is investigated, experimentally. The thermal and electrical outputs of the systems as the critical parameters are compared with each other and with those of a conventional similar

Table 6
Summary of systems exergy.

System type	PV	PVT		PVT/PCM	
Exergy		Deionized water	Nanofluid	Deionized water	Nanofluid
Input exergy (Sun) (W/m^2)	845.42	845.42	845.42	845.42	845.42
Thermal exergy output (W/m^2)	0	4.21	4.35	7.37	9.11
Electrical exergy output (W/m^2)	92.16	99.23	99.63	103.99	104.4
Total exergy output (W/m^2)	92.16	103.44	103.98	111.36	113.51
Overall exergy efficiency (%)	10.9	12.23	12.29	13.17	13.42

photovoltaic module as the reference system. Integrating the fluid based collector of the PVT system with a PCM medium is considered as a new approach that can improve the system performance. A *ZnO*/water nanofluid with 0.2 wt% is selected as a nanofluid coolant. The results for the surface temperature measurement showed that using a fluid (deionized water or nanofluid) as coolant for the PVT system, can reduce the cell temperature by about 10 degrees (in average) during a work cycle period (9:30 am −15:30 pm). The cell temperature reduction of the PVT fluid/nanofluid coolant system with a PCM medium is more than 16 degrees compared to that of the reference system in the same condition. Also, it is concluded that for the PCM/nanofluid based collector system, the average electrical output is increased by about 13% in comparison with the conventional PV module. Moreover, the average thermal energy output of the PCM/water based collector is increased by 42% in comparison with the case of the water based collector without a PCM medium. This value is about 48% for the case of PCM/nanofluid based collector in comparison with the case of the nanofluid based collector. From the exergy analysis results, it is found that in the PVT fluid/nanofluid based collector system with the PCM medium, the overall exergy efficiency of the system is increased more than 23%, in comparison with a conventional PV system. In conclusion, a PCM medium without any extra energy consumption can be a suitable option to improve the cooling in a PVT system significantly.

Acknowledgements

The financial support of the Air and Solar Research Institute of the Ferdowsi University of Mashhad is gratefully acknowledged.

References

[1] M. Sardarabadi, M. Passandideh-Fard, S. Zeinali Heris, Experimental investigation of the effects of silica/water nanofluid on PV/T (photovoltaic thermal units), Energy 66 (2014) 264–272.
[2] A. Hasan, S.J. McCormack, B. Norton, Evaluation of phase change materials for thermal regulation enhancement of building integrated photovoltaics, Sol. Energy 84 (2010) 1601–1612.
[3] M.J. Huang, P.C. Eames, B. Norton, N.J. Hewitt, Natural convection in an internally finned phase change material heat sink for the thermal management of photovoltaics, Sol. Energy Mater. Sol. Cells 95 (2011) 1598–1603.
[4] A. Hasan, S.J. McCormack, M.J. Huang, J. Sarwar, B. Norton, Increased photovoltaic performance through temperature regulation by phase change materials: materials comparison in different climates, Sol. Energy 115 (2015) 264–276.
[5] T. Ma, H. Yang, Y. Zhang, L. Lu, X. Wang, Using phase change materials in photovoltaic systems for thermal regulation and electrical efficiency improvement: a review and outlook, Renew. Sustain. Energy Rev. 43 (2015) 1273–1284.
[6] M.C. Browne, B. Norton, B.C. McCormack, Phase change materials for photovoltaic thermal management, Renew. Sustain. Energy Rev. 47 (2015) 762–782.
[7] K. Touafek, A. Khelifa, M. Adouane, Theoretical and experimental study of sheet and tubes hybrid PVT collector, Energy Convers. Manag. 80 (2014) 71–77.
[8] M. Moradgholi, S.M. Nowee, I. Abrishamchi, Application of heat pipe in an experimental investigation on a novel photovoltaic/thermal (PV/T) system, Sol. Energy 107 (2014) 82–88.
[9] M. Farshchimonfared, J.I. Bilbao, A.B. Sproul, Channel depth, air mass flow rate and air distribution duct diameter optimization of photovoltaic thermal (PV/T) air collectors linked to residential buildings, Renew. Energy 76 (2015) 27–35.
[10] J. Yazdanpanahi, F. Sarhaddi, M. Mahdavi-Adeli, Experimental investigation of exergy efficiency of a solar photovoltaic thermal (PVT) water collector based on exergy losses, Sol. Energy 118 (2015) 197–208.
[11] Y.N. Tripanagnostopoulos, T.M. Souliotis, P. Yianoulis, Hybrid photovoltaic/thermal solar systems, Sol. Energy 72 (2002) 217–234.
[12] A. Kasaeian, A. Toghi-Eshghi, M. Sameti, A review on the applications of nanofluids in solar energy systems, Renew. Sustain. Energy Rev. 43 (2015) 584–598.
[13] J.J. Michael, S. Iniyan, Performance analysis of a copper sheet laminated photovoltaic thermal collector using copper oxide – water, Sol. Energy 119 (2015) 439–451.
[14] M. Ghadiri, M. Sardarabadi, M. Pasandideh-fard, A. Jabari Moghadam, Experimental investigation of a PVT system performance using nano ferrofluids, Energy Convers. Manag. 103 (2015) 468–476.
[15] O. Rejeb, M. Sardarabadi, C. Ménézo, M. Pasandideh-fard, M.H. Dhaou, A. Jemni, Numerical and model validation of uncovered nanofluid sheet and tube type photovoltaic thermal solar system, Energy Convers. Manag. 110 (2016) 367–377.
[16] S.K. Verma, A.K. Tiwari, Progress of nanofluid application in solar collectors: a review, Energy Convers. Manag. 100 (2015) 324–346.
[17] A. Najah Al-Shamani, M.H. Yazdi, M.A. Alghoul, A.M. Abed, M.H. Ruslan, S. Mat, K. Sopian, Nanofluids for improved efficiency in cooling solar collectors – A review, Renew. Sustain. Energy Rev. 38 (2014) 348–367.
[18] Diracdelta.co.uk, Science and Engineering Encyclopedia. Dirac Delta Consultants Ltd, Warwick, England, Retrieved June 2016, ⟨http://www.diracdelta.co.uk⟩.
[19] H. Chemming, M. Richard, Solar cells from basic to advanced systems., McGraw Hill, University of California, 1930.
[20] A. Bejan, Entropy generation minimization, Wiley, New York, 1982.
[21] S.J. Kline, F.A. McClintock, Describing uncertainties in single-sample experiments, Mech. Eng. 75 (1953) 3–8.
[22] J.R. Taylor, An introduction to error analysis: the study of uncertainties in physical measurements, Sausalito, University Science Books, 1997.